RSC Advances

PAPER

View Article Online
View Journal | View Issue

Cite this: *RSC Adv.*, 2025, **15**, 22661

A DFT/TD-DFT investigation of clozapine adsorption on $B_{12}Y_{12}$ (Y = N, P) nanocages as vehicles for applications in schizophrenia treatment†

Charly Tedjeuguim Tsapi,[a] Stanley Numbonui Tasheh,[b]* Aymard Didier Tamafo Fouegue,[c] Numbonui Angela Beri,[b] Caryne Isabelle Lekeufack Alongamo,[a] Emmanuel Dassi Atongo[d] and Julius Numbonui Ghogomu[ab]*

Clozapine (**Clo**) is a highly effective antipsychotic for treatment-resistant schizophrenia, but its clinical use is hampered by poor delivery due to its lipophilic nature. In this study, density functional theory (DFT) and time-dependent DFT (TD-DFT) were used to investigate $B_{12}N_{12}$ and $B_{12}P_{12}$ nanocages as potential carriers for **Clo** delivery. Molecular electrostatic potential (MEP) analysis revealed three electron-rich adsorption sites on **Clo** (N13, Cl16, and N32), which served as anchoring points for nanocage attachment. **Clo**/$B_{12}N_{12}$ configurations (**A–C**) and **Clo**/$B_{12}P_{12}$ complexes (**D–F**) were labelled as Sites 1–3. The findings reveal that the adsorption energies for **Clo** on both nanocages fall between −20 and −40 kcal mol^{-1} (*i.e.* −39.96 to −22.05 kcal mol^{-1}), indicating strong and stable chemisorption. These interactions are both spontaneous and exothermic, as supported by negative values of ΔG_{ad} and ΔH_{ad}. NBO analysis demonstrates greater charge transfer from **Clo** to $B_{12}N_{12}$ (up to 1.240*e*) compared to $B_{12}P_{12}$ (up to 0.589*e*). Both nanocages significantly reduce the HOMO–LUMO gap of the system (by 42.66% for $B_{12}N_{12}$ and 29.52% for $B_{12}P_{12}$), which enhances conductivity and could facilitate drug detection. QTAIM analysis indicates that complexes **A**, **C**, **D** and **F** feature partially covalent interactions, while **B** and **E** are more ionic, suggesting a balance between strong binding and the potential for controlled release. Recovery time calculations further show that complexes **B** and **E** allow for faster drug release. Overall, these findings highlight $B_{12}N_{12}$ and $B_{12}P_{12}$ nanocages as promising nanocarriers for targeted clozapine delivery, combining stable binding with the potential for efficient and controlled drug release and, however, warranting experimental validation for addressing current challenges in schizophrenia therapy.

Received 19th April 2025
Accepted 21st June 2025

DOI: 10.1039/d5ra02752g

rsc.li/rsc-advances

1. Introduction

Nanotechnology has revolutionized the healthcare industry in recent years, particularly in drug delivery within biological systems.[1,2] Among the most practical methods, the use of nanocages has proven highly effective for delivering drugs into the human body.[3] Boron nitride $(BN)_n$ and boron phosphide $(BP)_n$ nanocages stand out due to their unique properties, encompassing high hardness, low thermal expansion, excellent thermal conductivity and semiconductor properties alongside specific chemical and physical qualities. These attributes make them ideal for electronic applications as well as for use as sensors or adsorbents for various toxic and medicinal compounds.[4,5]

Research into the computational properties of different $(XY)_n$ nanocages (where X = B, Al, *etc.*, and Y = N, P, *etc.*) has revealed that the most stable configuration is the $X_{12}Y_{12}$ fullerene-like nanocage structure.[1] Significant attention has been devoted to studying the adsorption behaviour of various systems on the surface of $B_{12}N_{12}$ and $B_{12}P_{12}$ nanocages. For instance, $B_{12}N_{12}$ has been shown to effectively adsorb compounds such as

[a]*Research Unit of Noxious Chemistry and Environmental Engineering, Department of Chemistry, Faculty of Science, University of Dschang, P.O. Box 67, Dschang, Cameroon. E-mail: ghogsjuju@hotmail.com*

[b]*Department of Chemistry, Faculty of Science, The University of Bamenda, P.O. Box 39 Bambili, Bamenda, Cameroon. E-mail: tashehstanley@uniba.cm*

[c]*Department of Chemistry, Higher Teacher Training College Bertoua, University of Bertoua, P.O Box 652, Bertoua, Cameroon*

[d]*School of Chemical and Biomolecular Sciences, Southern Illinois University Carbondale, IL, 62901, USA*

† Electronic supplementary information (ESI) available: The ESI comprises additional tables constituting part of this work. Tables S1–S9 are the cartesian coordinates of the studied compounds, Table S10 is the NBO data of the complexes and Fig. S1 is the calculated absorption spectra of the investigated molecules. See DOI: https://doi.org/10.1039/d5ra02752g

allopurinol,[6] chloropicrin,[7] N-(4-methoxybenzylidene)isonicotinohydrazone,[8] mercaptopurine,[9] trinitroanisole,[10] cysteine,[11] paracetamol,[12] melphalan[13] and the herbicide glyphosate.[14] Similarly, the $B_{12}P_{12}$ nanocage has demonstrated adsorption capabilities for compounds like valproic acid,[1] 5-fluorouracil,[15] thiophene,[16] dimethyl ether,[17] guanine[18] and bendamustine.[19] Furthermore, the therapeutic potential of boron clusters in drug delivery and cancer therapy is becoming well documented.[9,13,19] Moreover, quetiapine recognized for its neurological benefits, has been successfully adsorbed onto $B_{12}N_{12}$ nanocages for the treatment of schizophrenia and the results indicate that $B_{12}N_{12}$ is an effective adsorbent for the delivery of quetiapine, offering promising potential for advanced drug delivery systems.[20]

Schizophrenia, which affects ~1% of the global population, necessitates effective antipsychotic therapies to address its complex and debilitating symptoms.[21] Among these, **Clo** (see Fig. 1 for its structure) stands out as the most effective treatment for refractory schizophrenia.[22] While it remains unmatched in managing treatment-resistant cases, clozapine's high lipophilicity poses significant challenges. This property not only reduces its bioavailability but also necessitates frequent dosing, which increases the risk of severe side effects, such as agranulocytosis.[21,23]

In light of these challenges, nanotechnology emerges as a promising solution for enhancing drug delivery. However, the absence of specifically designed nanocarriers for clozapine hinders its clinical optimization.[24] To address this gap, this study explores the potential of pure $B_{12}N_{12}$ and $B_{12}P_{12}$ nanocages as innovative nano vehicles for delivering clozapine, employing methodologies based on density functional theory (DFT) and its time-dependent extension (TD-DFT). These investigations focus on computing key properties such as the thermodynamic, geometrical, UV-Vis spectrum, QTAIM and density of states (DOS) spectra. Equally, frontier molecular orbital (FMO) and natural bond orbital (NBO) analyses were evaluated. The findings obtained from this research have the potential to revolutionize drug delivery for clozapine by enabling the development of advanced medication delivery systems or drug sensors tailored for biological applications.

2. Computational details

This study investigates the interactions between **Clo** and $B_{12}N_{12}$/$B_{12}P_{12}$ nanocages using DFT. Quantum calculations were performed with Gaussian 09 (Revision D.01),[25] while molecular model preparations and result visualizations were assessed using GaussView 6.0.16.[26] The geometries of **Clo**, the nanocages and the resulting complexes were refined with the B3LYP functional attached to the 6-311G(d,p) basis set.[27,28] To enhance accuracy, Grimme's D3 dispersion corrections were incorporated to account for long-range van der Waals interactions.[29] Frequency calculations confirmed system stability by the absence of imaginary frequencies, ensuring that each nanocage resides in an energy-minimized state.

Gauss Sum software[30] generated density of states (DOS) diagrams to map orbital contributions. For modelling excited-state behaviour, TD-DFT was conducted with the CAM-B3LYP/6-311G(d,p) theoretical level,[31] capturing electronic transitions. Interatomic interactions were obtained using Multiwfn

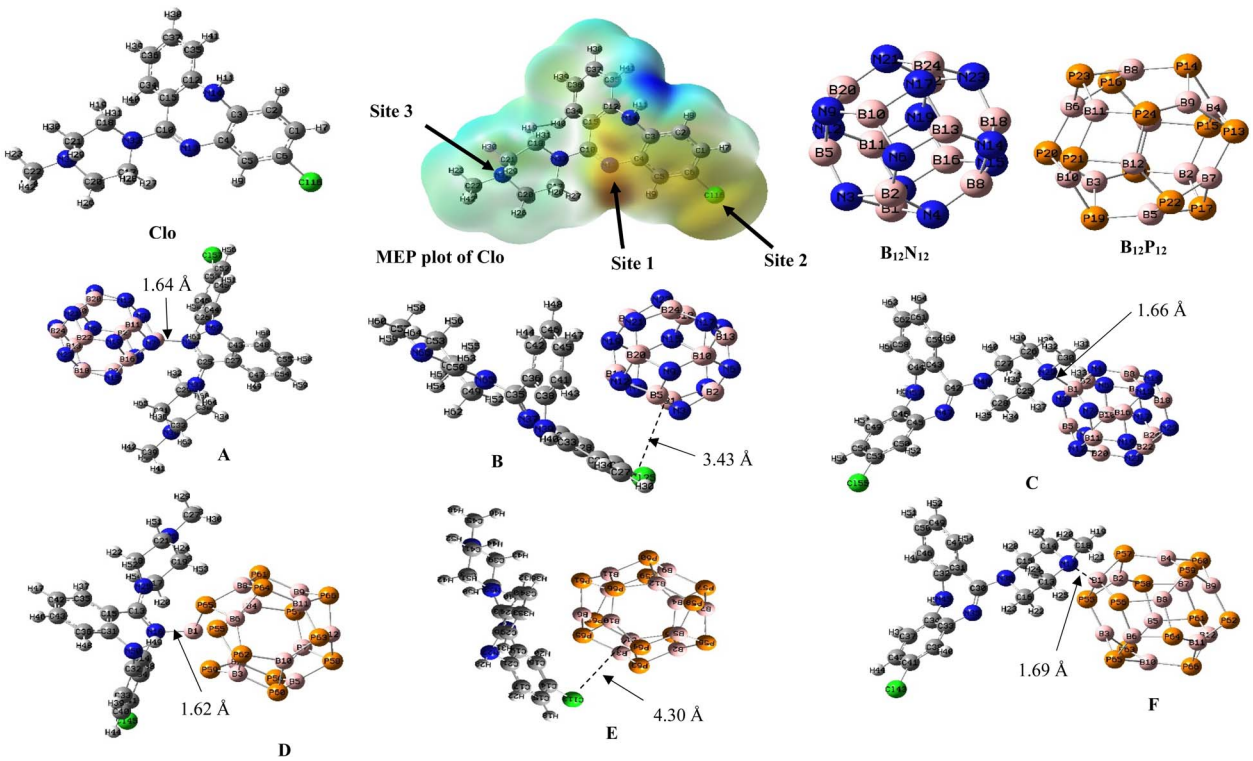

Fig. 1 MEP plot of **Clo** and the minimized structures of the investigated compounds.

3.3.7 (ref. 32) *via* the quantum theory of atoms in molecules (QTAIM), revealing bond critical points. Mindful of the possibility of superposition errors in computations involving the molecules interacting, basis set superposition errors (BSSE) were mitigated making use of the counterpoise method, to ensure accuracy in adsorption energy calculations.[33,34] Finally, natural bond orbital (NBO) analysis, integrated within the Gaussian 09 framework,[25] probed charge transfer and hybridization effects at the B3LYP/6-311G(d,p) level.

Key thermodynamic metrics like the enthalpy change (ΔH_{ad}), adsorption energy (E_{ad}), Gibbs free energy change (ΔG_{ad}) and entropy change (ΔS_{ad}) for the compounds under investigation were calculated under standard conditions (1 atm and 298.15 K) using the following equations.[6] These parameters provide crucial insights into the stability and spontaneity of the adsorption processes.

$$\text{clozapine} + \text{nanocage} \rightarrow \text{clozapine–nanocage} \quad (1)$$

$$E_{ad} = E_{\text{clozapine–nanocage}} - (E_{\text{clozapine}} + E_{\text{nanocage}}) \quad (2)$$

$$E_{ad}^{CP} = E_{ad} + E_{BSSE} \quad (3)$$

$$\Delta H_{ad} = H_{\text{clozapine–nanocage}} - (H_{\text{clozapine}} + H_{\text{nanocage}}) \quad (4)$$

$$\Delta S_{ad} = S_{\text{clozapine–nanocage}} - (S_{\text{clozapine}} + S_{\text{nanocage}}) \quad (5)$$

$$\Delta G_{ad} = \Delta H_{ad} - T\Delta S_{ad} \quad (6)$$

The variables G, H, E, S and T above stand for the Gibbs free energy, enthalpy, total electronic energy (ZPE + electronic), entropy and temperature.

Furthermore, electronic descriptors including band gaps (E_{gap}), band gap variation ($\%\Delta E_{gap}$), chemical hardness (η), softness (σ), fermi level energy (E_{FL})[24] and work function (Φ) were determined to assess the reactivity and stability of the systems according to the following equations:[35,36]

$$E_{gap} = E_L - E_H \quad (7)$$

$$\%\Delta E_{gap} = \frac{E_{gap_{\text{clozapine–nanocage}}} - E_{gap_{\text{nanocage}}}}{E_{gap_{\text{nanocage}}}} \times 100 \quad (8)$$

$$\eta = \frac{(E_L - E_H)}{2} \quad (9)$$

$$\sigma = \frac{1}{2\eta} \quad (10)$$

$$E_{FL} = E_H + \frac{\Delta E_g}{2} \quad (11)$$

$$\Phi = V_{el(+\infty)} - E_{FL} \quad (12)$$

E_H and E_L represent the energy of the highest occupied molecular orbital (HOMO) and the lowest unoccupied molecular orbital (LUMO), respectively.[37] The electrostatic potential of the material surface is represented by $V_{el(+\infty)}$, which appears to be lowered to zero.[7]

3. Results and discussion

3.1. Structural analysis, adsorption energy and thermodynamic properties

Fig. 1 illustrates the optimized geometries of clozapine (**Clo**), pristine $\mathbf{B_{12}N_{12}}$ and $\mathbf{B_{12}P_{12}}$ nanocages and their corresponding **Clo**–nanocage complexes. To identify preferential adsorption sites on **Clo**, its molecular electrostatic potential (MEP) map post-optimization was analysed (see Fig. 1). The MEP plot revealed three electron-rich regions localized on atoms N13 (Site 1), Cl16 (Site 2), and N32 (Site 3), which served as nucleophilic centres for nanocage interactions. Based on these sites, **Clo**/$\mathbf{B_{12}N_{12}}$ nanocage complexes were labelled **A** (Site 1), **B** (Site 2) and **C** (Site 3), while the **Clo**/$\mathbf{B_{12}P_{12}}$ complexes were designated **D**, **E** and **F** corresponding to the same sites, respectively. Listed in Tables S1–S9 of the attached ESI† are the Cartesian coordinates for all optimized systems.

The optimized geometries of the clozapine–nanocage complexes revealed varying minimal interaction distances between the adsorbate (clozapine) and the adsorbents ($\mathbf{B_{12}N_{12}}$ and $\mathbf{B_{12}P_{12}}$ nanocages). Specifically, the interaction distances were measured as the shortest equilibrium bond lengths between clozapine's N13, Cl16, and N32 atoms (at Sites 1–3) and the nanocage's boron atom, based on DFT-optimized geometries. These distances were calculated as 1.62 Å, 1.64 Å, 1.66 Å, 1.69 Å, 3.63 Å and 4.30 Å for **D**, **A**, **C**, **F**, **B** and **E**, respectively. The shorter interaction distances observed in complexes **D**, **A**, **C** and **F** suggest stronger interactions that favour chemisorption, while the longer distances in complexes **B** and **E** indicate weaker interactions more characteristic of physisorption.

As mentioned earlier, all calculated frequencies are positive (Table 1). The stretching modes of the B–N bonds (representing the **Clo**/nanocages interaction) in complexes **A**, **C**, **D** and **F** were approximately 756.86 cm^{-1}, 767.28 cm^{-1}, 734.34 cm^{-1}, and 611.47 cm^{-1}, respectively. These values confirm the formation of new B–N bonds and indicate strong interactions between clozapine and these nanocages. In contrast, for complexes **B** and **E**, a B–Cl stretching mode was observed instead of a B–N bond formation. This suggests that the interactions in these complexes are weaker and primarily involve a B–Cl bond rather than chemisorption.

Table 1 equally presents adsorption energy (E_{ad}), enthalpy variation (ΔH_{ad}), Gibbs free energy variations (ΔG_{ad}) and entropy variation (ΔS_{ad}) values, used to understand the thermodynamics of **Clo**'s adsorption process at the exterior surface of the $\mathbf{B_{12}N_{12}}$ and $\mathbf{B_{12}P_{12}}$ nanocage.

The adsorption energies (E_{ads}) of **Clo** on $\mathbf{B_{12}N_{12}}$ and $\mathbf{B_{12}P_{12}}$ nanocages reveal thermodynamically favourable interactions across all studied complexes, as indicated by their negative values. Without basis set superposition error (BSSE) correction, the stability order follows: **C** > **A** = **D** = **F** > **B** = **E**, with values ranging from −43.92 to −25.10 kcal mol^{-1}. When accounting for BSSE, the stability sequence adjusts to: **C** > **F** > **A** > **D** > **E** > **B**, with corrected values between −39.96 and −22.05 kcal mol^{-1}. The obtained range of adsorbed energies aligns with chemisorption

Table 1 Thermodynamic parameters, minimum and maximum vibrational frequencies for the reported systems[a]

Systems	d	ν_{min}	ν_{max}	ν_{B-N}	E_{ad}^{b}	E_{BSSE}^{b}	$E_{ad}^{CP^b}$	ΔH_{ad}^{b}	ΔS_{ad}^{b}	ΔG_{ad}^{b}	τ
Clozapine	—	8.66	3563.41	—	—	—	—	—	—	—	—
$B_{12}N_{12}$	—	327.10	1436.50	—	—	—	—	—	—	—	—
A	1.64	17.55	3391.16	756.86	−31.37	4.18	−27.19	−31.37	−0.052	−15.86	635×10^5
B	3.43	9.80	3560.42	—	−25.10	3.05	−22.05	−25.10	−0.042	−12.58	114×10^2
C	1.66	11.67	3568.34	767.28	−43.92	3.96	−39.96	−43.92	−0.052	−28.42	126×10^{15}
$B_{12}P_{12}$	—	151.92	911.30	—	—	—	—	—	—	—	—
D	1.62	10.33	3478.88	734.34	−31.37	4.48	−26.89	−37.67	−0.052	−22.17	384×10^5
E	4.30	12.50	3564.09	—	−25.10	2.72	−22.38	−37.67	−0.044	−24.56	199×10^2
F	1.69	9.99	3570.05	611.47	−31.37	4.07	−27.30	−31.37	−0.052	−15.87	763×10^5

[a] d → adsorbate–adsorbent distance (Å), ν_{min} → minimum frequencies (cm^{-1}), ν_{max} → maximum frequencies (cm^{-1}), $\nu_{B-}N$ → adsorbate–adsorbent frequencies (cm^{-1}), E_{ad}^{b} → adsorption energy, ΔH_{ad}^{b} → enthalpy change, ΔS_{ad}^{b} → entropy change, ΔG_{ad}^{b} → Gibbs free energy change, E_{BSSE}^{b} → basis set superposition error,τ → recovery time (s); [b]: units in kcal mol^{-1}; $E_{ad}^{CP^b}$ → counterpoise corrected adsorption energy.

threshold from a similar DFT study of drug adsorption onto boron-based or graphene-like nanostructures.[38]

Complex **C**, with the lowest adsorption energy (−39.96 kcal mol^{-1}), emerges as the most stable structure among all configurations, offering the optimal configuration for potential therapeutic applications. According to criteria established by Rakib and colleagues,[38] adsorption energies below −22.94 kcal mol^{-1} (−1 eV or −96 kJ mol^{-1}) indicate chemisorption rather than physisorption. The results therefore confirm that **Clo** undergoes chemisorption on the external surfaces of both nanocages, facilitated by charge transfer from the drug molecule to the nanocage structures. Notably, $B_{12}N_{12}$-based complexes demonstrate superior stability compared to their $B_{12}P_{12}$ counterparts, suggesting $B_{12}N_{12}$ nanocages may be more suitable candidates for clozapine delivery in schizophrenia treatment.

The negative enthalpy changes (ΔH) ranging from −43.92 to −25.10 kcal mol^{-1} indicate an exothermic adsorption process, releasing energy when **Clo** binds to the nanocage surfaces. Similarly, the Gibbs free energy changes (ΔG_{ads}) are consistently negative (−28.42 to −12.58 kcal mol^{-1}), confirming that complex formation occurs spontaneously and results in thermodynamically stable systems. These results are in-line with findings on similar works.[13,18] The entropy changes (ΔS_{ads}) are also negative across all complexes, suggesting that the interaction between clozapine (adsorbate) and the nanocages (adsorbents) creates a more ordered molecular arrangement at the binding interface.

To evaluate the practical utility of these carrier systems, the recovery time (τ) was evaluated, which estimates how quickly the drug molecule desorbs from the nanocage surface to perform its therapeutic action.[39] While complexes with higher adsorption energies demonstrate greater stability, they may face challenges in releasing the medication efficiently within biological systems.[39] Therefore, an optimal drug delivery system requires a balance between strong adsorption for stable transport and appropriate recovery time for effective drug release. The recovery times calculated at room temperature using eqn (13) are also listed in Table 1.

$$\tau = V_o^{-1} \exp\left(\frac{-E_{ad}^{CP}}{KT}\right) \quad (13)$$

where, V_o is the attempt frequency (10^{12} s^{-1}), E_{ad}^{CP} is the counterpoise corrected adsorption energy, T is the temperature (298.15 K), K is the Boltzmann constant (2×10^{-3} kcal mol^{-1} K^{-1}).[40]

According to Table 1, the recovery times for desorption of clozapine from the surfaces of $B_{12}N_{12}$ and $B_{12}P_{12}$ nanocages are in the order **C** > **F** > **A** > **D** > **E** > **B**. Based on these obtained recovery times, complexes **E** and **B** demonstrate shorter recovery times than the other complexes. As a result, **E** and **B** complexes are ideal carriers for clozapine delivery and can function as effective sensors for **Clo**.

3.2. Electronics properties (frontier molecular orbital analysis, DOS)

Table 2 presents the electronic parameters of the studied systems. The distribution of their frontier molecular orbitals is demonstrated in Fig. 2.

The results from the table reveals a significant decrease in the energy gap (E_{gap}) of the $B_{12}N_{12}$ and $B_{12}P_{12}$ nanocages upon the adsorption of clozapine under investigation. Specifically, before the adsorption of **Clo**, the $B_{12}N_{12}$ and $B_{12}P_{12}$ nanocages have E_{gap} values of 6.748 and 3.733 eV, respectively. Upon adsorption of **Clo**, their E_{gap} reduce by approximately 2.735 and 0.891 eV for, respectively, the $B_{12}N_{12}$–**Clo** and $B_{12}P_{12}$–**Clo** complexes. The increase in the order of conductivity according to the E_{gap} values of the studied compounds is: $B_{12}N_{12}$ < **B** < **C** < **A** < $B_{12}P_{12}$ < **F** < **D** < **E**. Moreover, a larger E_{gap} in a molecule generally leads to reduced chemical reactivity and enhanced stability. Notably, complex **E** exhibits the smallest energy gap, rendering it the most reactive among the investigated systems. A comparison of the $\Delta E_{gap}$of complexes **A**, **B** and **C** with that of the $B_{12}N_{12}$ nanocage, shows that the adsorption of **Clo** results in changes in the ΔE_{gap} values of approximately 39.22% to 42.66%. Similarly, comparing the ΔE_{gap} of the $B_{12}P_{12}$ nanocage with complexes **D**, **E** and **F** present changes of about 14.14% to 29.52%. This observation indicates that the adsorption of **Clo**

Table 2 Electronic parameters for the investigated systems computed at B3LYP-D/6-311G(d,p)[a]

Systems	E_H	E_L	E_{gap}	$\%E_{gap}$	E_{FL}	η	σ	Φ	DM
Clozapine	−5.418	−1.337	4.081	—	−3.37	2.04	0.245	3.37	5.17
$B_{12}N_{12}$	−7.855	−1.107	6.748	—	−4.48	3.37	0.148	4.48	0.00
A	−6.473	−2.604	3.869	42.66	−4.53	1.93	0.258	4.53	10.19
B	−5.584	−1.483	4.101	39.22	−3.53	2.05	0.243	3.53	4.89
C	−5.809	−1.741	4.068	39.71	−3.77	2.03	0.245	3.77	8.90
$B_{12}P_{12}$	−6.960	−3.227	3.733	—	−5.09	1.86	0.267	5.09	0.00
D	−5.688	−2.999	2.689	27.96	−4.34	1.34	0.371	4.34	12.40
E	−5.638	−3.007	2.631	29.52	−4.32	1.31	0.380	4.32	5.24
F	−5.892	−2.687	3.205	14.14	−4.28	1.60	0.312	4.28	10.58

[a] E_H: HOMO energy (eV), E_L: LUMO energy (eV), E_{gap}: energy gap (eV), $\%\Delta E_g$: percentage of the energy gap, E_{FL}: Fermi level energy (eV), η: chemical hardness (eV), σ: chemical softness (eV^{-1}), Φ: work function (eV), DM: dipole moment (debye).

significantly affects E_{gap} and enhances the conductivity of the nanocages. Density of states (DOS) analysis was employed to gain a more detailed understanding of the distribution of molecular orbitals in the examined systems. This analysis demonstrates a relationship between the frontier molecular orbitals and the HOMO/LUMO distribution.[41] The figure illustrates that the HOMO and LUMO densities of the nanocages are uniformly dispersed.

The Fermi level energy (E_{FL}) of the reported systems increases from −4.48 eV in the pure $B_{12}N_{12}$ nanocage to −3.53 eV and −3.77 eV in complexes **B** and **C**, respectively. Similarly, the E_{FL} of the considered systems increases from −5.09 eV in the pure $B_{12}P_{12}$ nanocage to −4.34 eV, −4.32 eV and −4.28 eV in complexes **D**, **E** and **F**, respectively. **Clo**'s adsorption increases the E_{FL} and decreases the work function (Φ), which is crucial for field emission applications.

For the assessed complexes, Φ decreases from 4.48 eV in pure $B_{12}N_{12}$ to 3.53 and 3.77 eV in complexes **B** and **C**, respectively, while it decreases from 5.09 eV in pure $B_{12}P_{12}$ to 4.34, 4.32 and 4.28 eV in complexes **D**, **E** and **F**, respectively. The outcomes demonstrate that **Clo** adsorption facilitates the field emission characteristics. Soft molecules have the highest reactivity due to their low chemical hardness (η) value. In the present study, η decreases upon adsorption and increases the reactivity of the complexes. The η values of all examined compounds vary from 1.31–3.37 eV. Complex **E** has the lowest η values of all of these compounds, making it the most reactive.

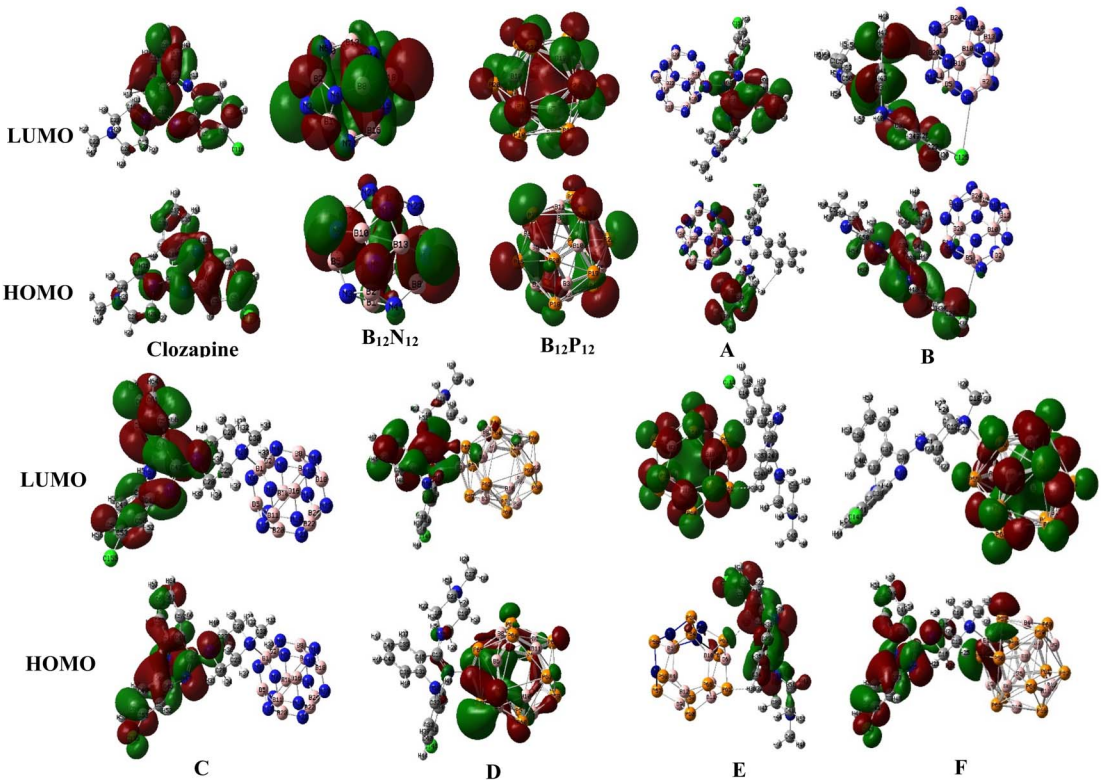

Fig. 2 The HOMO and LUMO orbitals of clozapine drug adsorbed on the surface of $B_{12}N_{12}$ and $B_{12}P_{12}$ nanocages.

The data in Table 2 equally informs that the dipole moments (DMs) of both nanocages are 0.00 debye, resulting from their symmetric nature. However, upon the adsorption of **Clo**, the DMs significantly increase. The DM of all studied complexes spans from 4.89 to 12.40 debye. This change in DM also indicates a charge transfer between **Clo** and the $B_{12}N_{12}$/$B_{12}P_{12}$ nanocages. Among these configurations, complex **E** exhibits the highest DM. This finding suggests that the adsorption of **Clo** enhances the polarity of the nanocages.

Fig. 2 illustrates the HOMO and LUMO distributions of all the studied systems. The HOMO represents the region where electrons are readily available for donation, while the LUMOs, represent the area which accommodates electrons. The results show that the HOMO and LUMO orbitals of **Clo** and free nanocages ($B_{12}N_{12}$ and $B_{12}P_{12}$) are evenly distributed overall the molecules. As observed in the figure, the HOMOs of all the investigated complexes are distributed on the tricyclic benzodiazepine group except in complex **A** which is located in the methylpiperazine group and complex **D** which is located in adsorbent group. The LUMO are also located on the tricyclic benzodiazepine group for complexes **A**, **B**, **C**, **D**. The LUMO is also observed in adsorbent group for **E** and **F** complexes. In general, for complexes **A**, **B** and **C**, the HOMO and LUMO orbitals are located on **Clo**, principally on the tricyclic benzodiazepine group, whereas for complexes **D**, **E** and **F** they are distributed across both **Clo** and the nanocages.

The energy gap of the systems can equally be presented using the DOS spectra.[42] The DOS plots indicate that the adsorption of **Clo** causes changes in the electronic properties of the pure nanocages (see Fig. 3). They show that a decrease in the energy gap is caused by an increase in the population of conduction electrons, which can produce an electrical signal. As a result, **Clo** can be identified by $B_{12}N_{12}$ and $B_{12}P_{12}$ nanocages.

Table 3 QTAIM metrics for the **Clo**/nanocages interactions investigated at B3LYP-D3/6-311G(d,p) level[a]

Systems	Bond	$\rho(r)$	$\nabla^2\rho(r)$	$H(r)$	$G(r)$	$V(r)$	$-G(r)/V(r)$
A	B–N	0.118	0.200	−0.884	0.138	−0.227	0.607
B	N–Cl	0.0052	0.017	0.0009	0.0034	−0.0024	1.416
C	B–N	0.119	0.171	−0.913	0.134	−0.225	0.595
D	B–N	0.121	0.252	−0.889	0.153	−0.242	0.632
E	P–Cl	0.0041	0.012	0.0007	0.0023	−0.0015	1.533
F	B–N	0.110	0.177	−0.080	0.125	−0.206	0.606

[a] $\rho(r)$ → total electronic densities, $\nabla^2\rho(r)$ → Laplacian of electron densities, $H(r)$ → total electronic energy, $V(r)$ → the potential energy, $G(r)$ → kinetic energy.

3.3. Quantum theory of atoms in molecules (QTAIM) analysis

To determine the types of interactions between clozapine (**Clo**) and the nanocages, Bader's topological approach was employed.[43] This method involves calculating key Quantum Theory of Atoms in Molecules (QTAIM) parameters at the bond critical points (BCPs) for all studied complexes. These parameters include the Laplacian of electron density ($\nabla^2\rho(r)$), electron density ($\rho(r)$), electronic energy density ($H(r)$), potential energy density ($V(r)$), and kinetic energy density ($G(r)$).[44] According to Cremer and collaborators[45] a positive $H(r)$ value typically indicates non-covalent (electrostatic) interactions, while a negative $H(r)$ value suggests partially covalent interactions. Covalent bonds are generally characterized by $\rho(r) > 0.1$ a.u., $\nabla^2\rho(r) < 0$ a.u., and a $-G(r)/V(r)$ ratio < 1 a.u.[46] Partially covalent bonds are identified by $\rho(r) < 0.1$ a.u., $\nabla^2\rho(r) > 0$ a.u., and a $-G(r)/V(r)$ ratio between 0.5 and 1 a.u.[47] Non-covalent interactions (*e.g.*, ionic or van der Waals forces) are associated with $\rho(r) < 0.1$ a.u., $\nabla^2\rho(r) > 0$ a.u., and a $-G(r)/V(r)$ ratio > 1 a.u.[48] The calculated

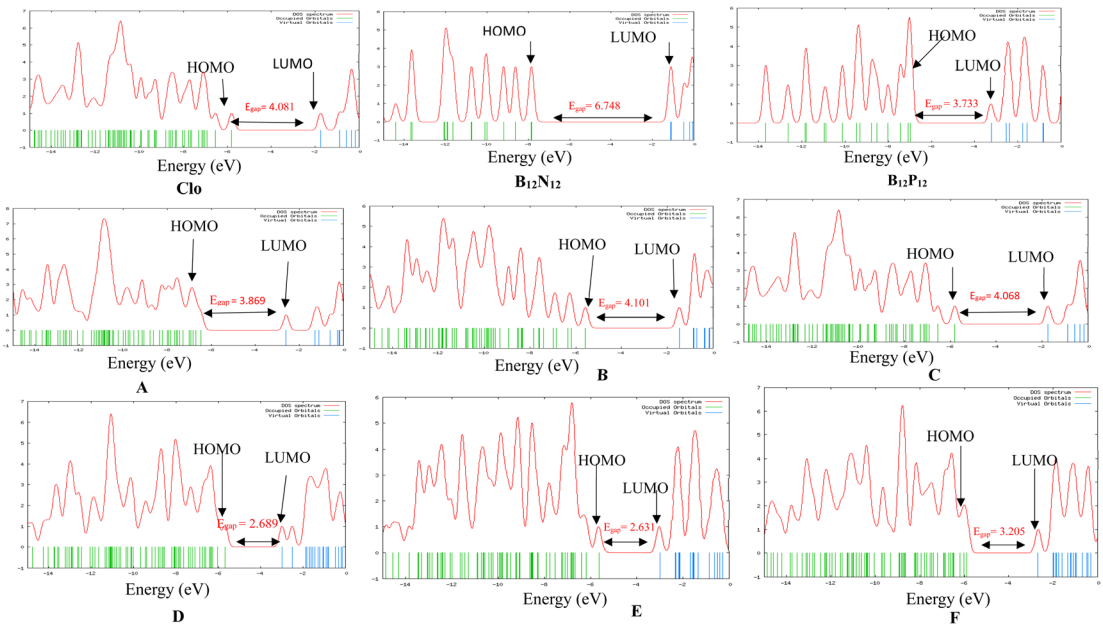

Fig. 3 Computed DOS plots of **Clo** adsorbed on $B_{12}N_{12}$ and $B_{12}P_{12}$ nanocages (systems A–F).

QTAIM metrics for the **Clo**/nanocages interactions are summarized in Table 3.

Table 3 shows that adsorbate–adsorbent bonds in **A**, **C**, **D** and **F** have negative $H(r)$ values, with positive $\nabla^2\rho(r)$ values, indicating medium interactions (partially covalent). In contrast, the H(r) and $\nabla^2\rho$(r) values of N–Cl (**B**) and P–Cl (**E**) bonds are positive, which confirms non-covalent bond interactions. The data also demonstrate that the adsorbate–adsorbent bonds have $-G(r)/V(r)$ values of 0.607; 0.595; 0.632, and 0.606 a.u. in **A**, **C**, **D** and **F**, respectively. These values, which fall between 0.5 and 1 a.u., are linked to partially covalent interactions. In contrast, the $-G(r)/V(r)$ values of N–Cl (**B**) and P–Cl (**E**) bonds are 1.416 and 1.533 a.u., confirming the non-covalent bond interactions. The use of QTAIM to differentiate partial covalency in **A**, **C**, **D** and **F** and ionic character in **B** and **E** adds depth to the bonding analysis. Such an approach has proven useful in understanding interaction types in host–guest chemistry and nanocarrier design.[49,50] The molecular graphs that indicate the bond critical point (BCP) of the interaction between clozapine and $\mathbf{B_{12}N_{12}}$ and $\mathbf{B_{12}P_{12}}$ nanocages is presented in Fig. S1 of the ESI data file.† The figure shows the presence of intermolecular interactions which tend to stabilize the complexes (Fig. 4).

3.4. NBO analysis

To analyse the charge transfer between clozapine (adsorbate) and the nanocages (adsorbents), Natural Bond Orbital (NBO) analysis was conducted at the same theoretical level. This analysis provides insights into the occupancy of donor and acceptor electrons and their stabilization energy, calculated using the second-order perturbation energy ($E^{(2)}$)[51–53] as:

$$E^{(2)} = q_i \frac{F_{ij}^{\ 2}}{\varepsilon_i - \varepsilon_j} \tag{14}$$

A higher $E^{(2)}$ value indicates a stronger adsorbate/adsorbent interaction, reflecting greater charge transfer and stabilization.[3] The results of this analysis are detailed in Table S10 of ESI,† offering a comprehensive understanding of the electronic interactions in the studied complexes.

The findings show that the donor–acceptor interaction energy of **Clo** complexes is related to the charge transfer from the nitrogen atom's bonding lone pair (LP) electrons and the boron atom's antibonding lone pair (LP*). The BD*(2) C52–C53 → BD*(2) C26–C46 interaction in **A** has the higher stabilization energy ($E^{(2)}$) about 323.00 kcal mol^{-1} compared to the BD*(2) C52–C53 → BD*(2) C44–C45, LP (1) N28 → LP*(2) B1, LP (2) N7 → LP*(1) B1 and LP (2) N4 → LP*(2) B1 interactions in the same complex. In **B**, the BD*(2) C26–C27 →BD*(2) C29–C33 interaction has a greater $E^{(2)}$ of approximately 349.72 kcal mol^{-1} compared to other interactions in the complex. The BD*(2) C53–C54 → BD*(2) C45–C50 interaction in **C** has a larger $E^{(2)}$ of about 267.68 kcal mol^{-1} compared to other interactions in the same complex. The BD*(2) C40–C41 → BD*(2) C32–C33 interaction in **D** has a higher $E^{(2)}$ of about 223.27 kcal mol^{-1} in comparison to the other interactions in the same complex. The BD*(2) C14–C15 → BD*(2) C16–C19 interaction in **E** has

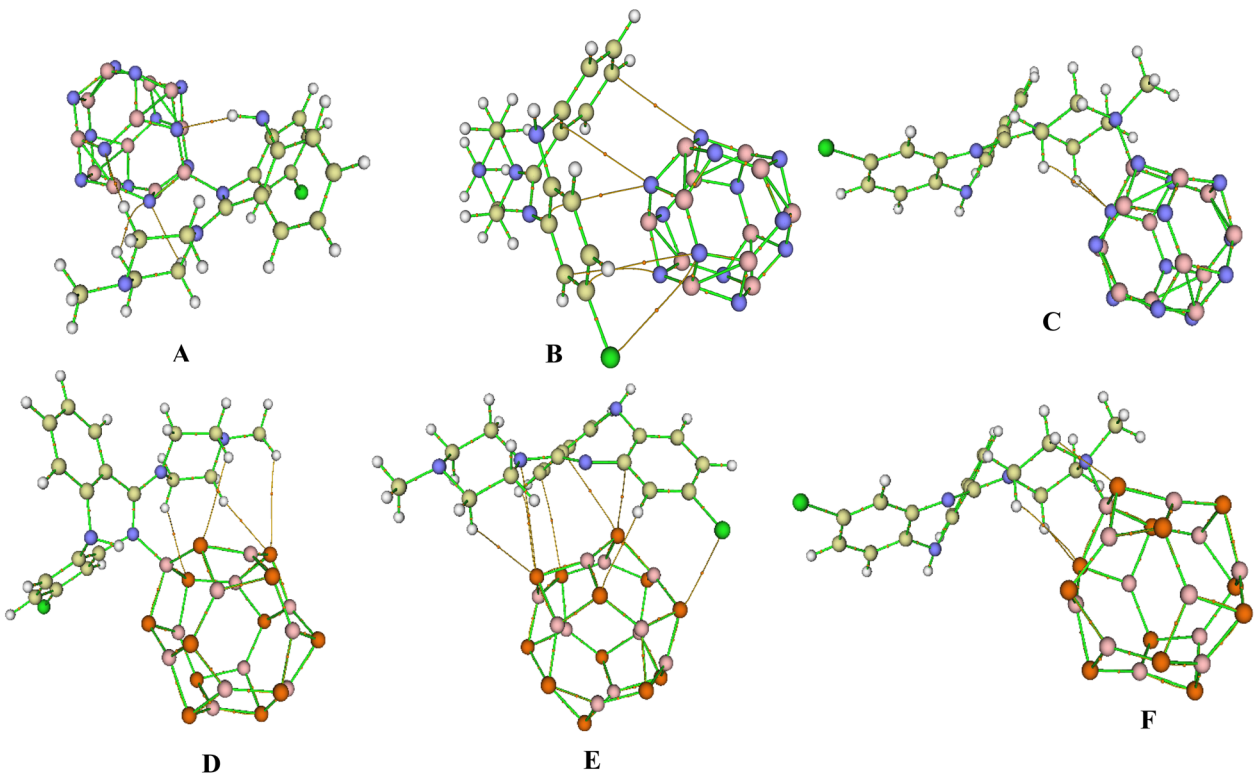

Fig. 4 Molecular graphs of the studied complexes.

Table 4 UV spectral parameters for the dominant electronic transitions of the investigated molecules obtained at CAM-B3LYP/6-311G(d,p) level of theory[a]

Systems	Excited state	MO + coefficient	E_{abs} (eV)	λ_{abs} (nm)	f
Clozapine	$S_0 \rightarrow S_{10}$	H-1 → L + 2 (36%)	5.96	208.01	0.25
$B_{12}N_{12}$	$S_0 \rightarrow S_1$	H → L (56%)	6.30	196.65	0.00
A	$S_0 \rightarrow S_1$	H-1 → L (48%)	4.34	285.26	0.15
B	$S_0 \rightarrow S_4$	H-3 → L (32%)	5.04	245.97	0.14
C	$S_0 \rightarrow S_9$	H-1 → L + 1 (51%)	6.01	206.26	0.29
$B_{12}P_{12}$	$S_0 \rightarrow S_{10}$	H → L + 2 (41%)	4.18	296.47	0.07
D	$S_0 \rightarrow S_3$	H-1 → L (59%)	3.37	367.88	0.02
E	$S_0 \rightarrow S_2$	H → L + 6 (55%)	3.67	337.04	0.04
F	$S_0 \rightarrow S_{10}$	H-2 → L + 1 (31%)	4.08	303.85	0.05

[a] E_{abs} → excitation energies (in eV), λ_{abs} → wavelengths (in nm), f → oscillator strengths, MO → molecular orbital coefficients, H → HOMO, L → LUMO.

a greater $E^{(2)}$ of 286.71 kcal mol^{-1} compared to other interactions in identical structures. The BD*(2) C41–C42 → BD*(2) C33–C38 interaction in **F** has a higher $E^{(2)}$ about 280.06 kcal-mol^{-1} in comparison to the other interactions in the same configuration. Among the studied complexes, **B** shows the highest stabilization energy (second-order perturbation energy $E^{(2)}$) and is probably the most stable compound.

Furthermore, to investigate the change in the electronic structure of nanocages produced by clozapine drug adsorption, we estimated the net charge transfer (Q_{NBO}) for all systems. The highest net charge transfer of complexes **A**, **B** and **C** were calculated as 1.172, 1.194 and 1.240*e*, respectively, while it is 0.589, 0.498 and 0.501*e* for complexes **D**, **E** and **F**, respectively. $B_{12}N_{12}$ nanocage complexes have high net charge transfer values as compared to their $B_{12}P_{12}$ counterparts, which is due to their high $E^{(2)}$ values. The higher charge transfer to $B_{12}N_{12}$ mirrors nitrogen-doped systems where N doping enhances electron-accepting potentials.[50]

3.5. UV spectral analysis

The excited states of the studied systems were analysed using TD-DFT at the CAM-B3LYP/6-311G(d,p) level. The first ten excited states were calculated for each system and the results are outlined in Table 4. This table includes the absorption wavelength (λ_{abs}), excitation energy (E_{abs}), oscillator strength, and orbital coefficients. Only the strongest bands, as indicated by their oscillator strengths are highlighted.

As observed in Table 4 (see Fig. S2 of ESI† for absorption spectra), all systems have wavelengths between 196.65 and 367.88 nm and oscillator strengths between 0.02 and 0.29. All of the investigated compounds are located in the UV region, which serves as the basis for this result. Results equally present a bathochromic shift upon the clozapine adsorption process on nanocages. The absorption energies range from 3.37 to 6.30 eV. Complexation decreases the excitation energy compared to pure nanocages and clozapine and this result is per the band gap energy of the studied compounds. A higher oscillator strength combined with lower transition energies results in a larger charge transfer. The increasing of λ_{max} values from the pure $B_{12}N_{12}$ (196.65 nm) to pure $B_{12}P_{12}$ (296.47 nm) reveals that $B_{12}P_{12}$ nanocage can be a suitable structure as an optic sensor for clozapine drug detection.

4. Conclusion

In this study, DFT and TD-DFT calculations were utilized to explore the adsorption of clozapine at the exterior surface of $B_{12}N_{12}$ and $B_{12}P_{12}$ nanocages. The results show that the molecular electrostatic potential (MEP) plot of the clozapine drug exhibits three preference electron-rich sites: N13 (Site 1), Cl16 (Site 2) and N32 (Site 3). The greatest adsorption energy in this study without counterpoise is in the range of −43.92 to −25.10 kcal mol^{-1}. The adsorption energy with counterpoise corrected (E_{ad}^{CP}) values of all complexes are in the range of −39.96 to −22.05 kcal mol^{-1}, supporting a chemisorption mechanism of clozapine drug at the external surface of the $B_{12}N_{12}$ and $B_{12}P_{12}$ nanocages. The ΔG_{ads} values of all the investigated complexes are also negative and range from −28.42 to −12.58 kcal mol^{-1}. Negative ΔG_{ads} values indicate that the investigated complexes form spontaneously and are thermodynamically stable. The dipole moments of all studied complexes are in the range of 4.89–12.40 debye respectively. Among these systems, complex **D** has the highest dipole moment. This result indicates that the adsorption of clozapine drug increases the polarity of nanocages. The DOS plots demonstrate that the adsorption significantly influenced the electronic density of states near the Fermi level and hence the conductivities of the systems increased. Quantum theory of atoms in molecules (QTAIM) analysis reveals that the interactions between the adsorbate and adsorbent are partially covalent and ionic in some cases. Based on the NBO analysis, there is charge transfer from clozapine molecule to nanocages in the complexes. All of these findings suggest that $B_{12}N_{12}$ and $B_{12}P_{12}$ nanocages can effectively adsorb the clozapine drug, making them viable nano vehicles for the neuroprotective medication. The findings from this study pave the way for experimental validation and a DFT study of the effect of solvents on the studied properties.

Data availability

The data to support the findings are existing in the manuscript and attached ESI file.†

Conflicts of interest

We declare we have no competing interests.

Acknowledgements

We received no funding for this study. We are grateful for the research support to lecturers of tertiary education by the Cameroonian Ministry of Higher Education.

References

1 J. S. Al-Otaibi, Y. S. Mary and Y. S. Mary, DFT analysis of valproic acid adsorption onto Al12/B12-N12/P12 nanocages with solvent effects, *J. Mol. Model.*, 2022, **28**, 98.
2 M. Reina, C. A. Celaya and J. Muñiz, C36 and C35E (E = N and B) Fullerenes as Potential Nanovehicles for Neuroprotective Drugs: A Comparative DFT Study, *ChemistrySelect*, 2021, **6**, 4844–4858.
3 M. Rezaei-Sameti and H. Zanganeh, TD-DFT, NBO, AIM, RDG and thermodynamic studies of interactions of 5-fluorouracil drug with pristine and P-doped Al12N12 nanocage, *Phys. Chem. Res.*, 2020, **8**, 511–527.
4 H. Ghasempour, M. Dehestani and S. M. A. Hossein, Theoretical studies of the paracetamol and phenacetin adsorption on single-wall boron-nitride nanotubes: a DFT and MD investigation, *Struct. Chem.*, 2020, **31**, 1403.
5 K. D. Karjabad, S. Mohajeri, A. Shamel, K. Moghaddam and G. E. Rajaei, Boron nitride nanoclusters as a sensor for Cyclosarin nerve agent: DFT and thermodynamics studies, *SN Appl. Sci.*, 2020, **2**, 574.
6 M. H. Miah, M. R. Hossain, M. S. Islam and T. F. F. Ahmed, A theoretical study of allopurinol drug sensing by carbon and boron nitride nanostructures: DFT, QTAIM, RDG, NBO and PCM insights, *RSC Adv.*, 2021, **11**, 38457.
7 A. A. Oishi, P. Dhali, A. Das, S. Mondal, A. S. Rad and M. M. Hasan, Study of the adsorption of chloropicrin on pure and Ga and Al doped B12N12: a comprehensive DFT and QTAIM investigation, *Mol. Simul.*, 2022, **48**, 776–788.
8 C. T. Tsapi, S. N. Tasheh, N. K. Nkungli, A. D. T. Fouegue, C. I. L. Alongamo and J. N. Ghogomu, Exohedral Adsorption of *N*-(4-methoxybenzylidene) Isonicotinohydrazone Molecule onto X12N12 Nanocages (where X = B and Al) and the Effect on Its NLO Properties by DFT and TD-DFT, *J. Chem.*, 2023, **2023**, 1–15.
9 N. M. Mahani, F. Mostaghni and H. Shafiekhani, A density functional theory study on the adsorption of Mercaptopurine anti-cancer drug and Cu/Zn-doped boron nitride nanocages as a drug delivery, *J. Biomol. Struct. Dyn.*, 2023, **42**, 1647.
10 M. R. J. Sarvestani and R. Ahmadi, Trinitroanisole adsorption on the surface of boron nitride nanocluster (B12N12): A Computational Study, *J. Water Environ. Nanotechnol.*, 2020, **5**, 34–44.
11 M. B. Javan, A. Soltani, E. T. Lemeski, A. Ahmadi and S. M. Rad, Interaction of B12N12 nano-cage with cysteine through various functionalities: A DFT study, *Superlattices Microstruct.*, 2016, **100**, 24–37.
12 S. Kainat, Q. Gul Ali, M. Khan, M. U. Rehman, M. Ibrahim, A. F. AlAsmari, F. Alasmari and M. Alharbi, Theoretical Modeling of B12N12 Nanocage for the Effective Removal of Paracetamol from Drinking Water, *Computation*, 2023, **11**, 183.
13 E. S. Mirkamali and R. Ahmadi, Adsorption of melphalan anticancer drug on the surface of boron nitride cage (B12N12): A comprehensive DFT study, *J. Med. Chem. Sci.*, 2020, **3**, 199–207.
14 O. V. Oliveira, J. D. Santos, J. C. F. Silva, L. T. Costa, M. F. F. Junior and E. F. Franca, Theoretical investigations of the herbicide glyphosate adsorption on the B12N12 nanocluster, *Electron. J. Chem.*, 2017, **9**, 175–180.
15 M. Rezaei-Sameti and A. Rezaei, A computational assessment of the interaction of 5Fluorouracil (5FU) drug connected to B12P12 and ScB11P12 nanocages with adenine nucleobase: DFT, AIM, TD-DFT study, *Struct. Chem.*, 2024, **35**, 105.
16 A. S. Rad and K. Ayub, Adsorption of thiophene on the surfaces of X12Y12 (X = Al, B, and Y = N, P) nanoclusters; A DFT study, *J. Mol. Liq.*, 2017, **238**, 303–309.
17 A. S. Rad, Comparison of X12Y12 (X = Al, B and Y = N, P) fullerene-like nanoclusters toward adsorption of dimethyl ether, *J. Theor. Comput. Chem.*, 2018, **17**, 1850013.
18 A. S. Rad and K. Ayub, A comparative density functional theory study of guanine chemisorption on Al12N12, Al12P12, B12N12, and B12P12 nano-cages, *J. Alloys Compd.*, 2016, **672**, 161–169.
19 N. M. Mahani, R. Behjatmanesh-Ardekani and R. Yosefelahi, Adsorption of bendamustine anti-cancer drug on Al/B–N/P nanocages: A comparative DFT study, *J. Serb. Chem. Soc.*, 2022, **87**, 1157–1170.
20 M. R. J. Sarvestani, M. G. Arashti and B. Mohasse, Quetiapine adsorption on the surface of boron nitride nanocage (B12N12): A computational study, *Int. J. New Chem.*, 2020, **7**, 87–100.
21 C. J. Wenthur and C. W. Lindsley, Classics in chemical neurosciences: clozapine, *ACS Chem. Neurosci.*, 2013, **4**, 1018–1025.
22 Y. Akamine, Y. Sugawara-Kikuchi, T. Uno, T. Shimizu and M. Miura, Quantification of the steady-state plasma concentrations of clozapine and *N*-desmethylclozapine in Japanese patients with schizophrenia using a novel HPLC method and the effects of CYPs and ABC transporters polymorphisms, *Ann. Clin. Biochem.*, 2017, **54**, 677–685.
23 C. F. Thorn, D. J. Müller, R. B. Altman and T. E. Klein, PharmGKB Summary: Clozapine Pathway, Pharmacokinetics, *Pharmacogenet. Genomics*, 2013, **28**, 214–222.
24 M. Kian and E. Tazikeh-Lemeski, B12Y (Y: N, P) fullerene-like cages for exemestane-delivery; molecular modeling investigation, *J. Mol. Struct.*, 2020, **1217**, 128455.
25 M. J. Frisch, G. W. Trucks, H. B. Schlegel, *et al.*, *Gaussian 09*, Gaussian Inc., Wallingford, CT, USA, 2009.

26 R. Dennington, T. A. Keith and J. M. Millam, *GaussView 6.0.1*, Semi chem Inc., Shawnee Mission, KS, 2016.
27 T. V. Russo, R. L. Martin and P. J. Hay, Density functional calculations on first-row transition metals, *J. Chem. Phys.*, 1994, **101**, 7729–7737.
28 R. Ditchfield, W. J. Hehre and J. A. Pople, Self-consistent molecular orbital methods: an extended gaussian-type basis for molecular orbital studies of organic molecules, *J. Chem. Phys.*, 1971, **54**, 724–728.
29 S. Grimme, J. Antony, S. Ehrlich and H. Krieg, A consistent and accurate *ab initio* parametrization of density functional dispersion correction (DFT-D) for the 94 elements H-Pu, *J. Chem. Phys.*, 2010, **132**, 154104.
30 N. M. O'Boyle, A. L. Tenderholt and K. M. Langner, A library for package-independent computational chemistry algorithms, *J. Comput. Chem.*, 2008, **29**, 839–845.
31 E. Lewars, *Computational Chemistry: Introduction to the Theory and Applications of Molecular and Quantum Mechanics*, Klumer Academy Publishers, New York, NY, USA, 2003.
32 T. Lu and F. C. Multiwfn, A multifunctional wavefunction analyser, *J. Comput. Chem.*, 2012, **33**, 580–592.
33 S. F. Boys and F. Bernardi, The calculation of small molecular interactions by the differences of separate total energies. Some procedures with reduced errors, *Mol. Phys.*, 1970, **19**, 553–566.
34 N. Abdolahi, M. Aghaei, A. Soltani, Z. Azmoodeh, Balakheyli and F. Heidari, Adsorption of Celecoxib on B12N12 fullerene: Spectroscopic and DFT/TD-DFT study, *Spectrochim. Acta, Part A*, 2018, **204**, 348–353.
35 R. G. Pearson, Absolute electronegativity and hardness: application to inorganic chemistry, *Inorg. Chem.*, 1988, **27**, 734–740.
36 P. Senet, Chemical hardnesses of atoms and molecules from frontier orbitals, *Chem. Phys. Lett.*, 1997, **275**, 527–532.
37 G. W. Ejuh, F. T. Nya, N. Djongyang and J. M. B. Ndjaka, Study of some properties of quinone derivatives from quantum chemical calculations, *Opt. Quantum Electron.*, 2018, **50**, 336.
38 H. M. Rakib, H. M. Mehade, N.-E. Ashrafi, *et al.*, Adsorption behaviour of metronidazole drug molecule on the surface of hydrogenated graphene, boron nitride and boron carbide nanosheets in gaseous and aqueous medium: A comparative DFT and QTAIM insight, *Phys. E*, 2021, **126**, 114483.
39 M. Sheikhi, S. Kaviani, F. Azarakhshi and S. Shahab, Superalkali X3O (X = Li, Na, K) doped B12N12 nano-cages as a new drug delivery platform for chlormethine: A DFT approach, *Comput. Theor. Chem.*, 2022, **1212**, 113722.
40 S. Peng, K. Cho, P. Qi and H. Dai, Ab initio study of CNT NO_2 gas sensor, *Phys. Lett.*, 2004, **387**, 271.
41 S. Hussain, S. A. S. Chatha, A. I. Hussain, R. Hussain, M. Y. Mehboob, A. Mansha, N. Shahzad and K. Ayub, In silico designing of $Mg_{12}O_{12}$ nanoclusters with a late transition metal for NO_2 adsorption: an efficient approach toward the development of NO_2 Sensing materials, *ACS Omega*, 2021, **6**, 14191–14199.
42 K. H. Hendriks, W. Li, M. M. Wienk and R. A. Janssen, Small-bandgap semiconducting polymers with high near-infrared photoresponse, *J. Am. Chem. Soc.*, 2014, **136**, 12130–12136.
43 R. F. W. Bader, *Atoms in Molecules: A Quantum Theory*, Oxford University Press, Oxford, 1990.
44 R. Bader, S. Anderson and A. Duke, Quantum topology of molecular charge distributions, *J. Am. Chem. Soc.*, 1979, **101**, 1389–1395.
45 D. Cremer and E. Kraka, Chemical bonds without bonding electron density-does the difference electron-density analysis suffice for a description of the chemical bond, *Angew Chem. Int. Ed. Engl.*, 1984, **23**, 627–628.
46 N. K. Nkungli and J. N. Ghogomu, Theoretical analysis of the binding of iron (III) protoporphyrin IX to 4-methoxyacetophenone thiosemicarbazone *via* DFT-D3, MEP, QTAIM, NCI, ELF, and LOL studies, *J. Mol. Model.*, 2017, **23**, 1–20.
47 G. V. Baryshnikov, B. F. Minaev, V. A. Minaeva, A. T. Podgornaya and H. Agren, Application of Bader's atoms in molecules theory to the description of coordination bonds in the complex compounds of Ca^{2+} and Mg^{2+} with methylidene rhodanine and its anion, *Russ. J. Gen. Chem.*, 2012, **82**, 1254–1262.
48 A. T. D. Fouegue, J. H. Nono, N. K. Nkungli and J. N. Ghogomu, A theoretical study of the structural and electronic properties of some titanocenes using DFT, TD-DFT, and QTAIM, *Struct. Chem.*, 2021, **32**, 353–356.
49 M. Khodiev, U. Holikulov, A. Jumabaev, N. Issaoui, L. N. Lvovich, O. M. Al-Dossary and L. G. Bousiakoug, Solvent effect on self-association of the 1,2,3-triazole: A DFT study, *J. Mol. Liq.*, 2023, **382**, 121960.
50 M. K. Khodiev, U. A. Holikulov, N. Issaoui, O. M. Al-Dossary, L. G. Bousiakoug and N. L. Lavrik, Estimation of electrostatic and covalent contributions to the enthalpy of H-bond formation in H-complexes of 1, 2, 3 benzotriazole with proton-acceptor molecules by IR spectroscopy and DFT calculations, *J. King Saud Univ., Sci.*, 2023, **35**, 102530.
51 E. Glendening, A. Reed, J. Carpenter & F. Weinhold, *NBO Version 3.1*, Gaussian Inc., Pittsburg, PA, CT, 2003.
52 M. Medimagh, N. Issaoui, S. Gatfaoui, O. Al-Dossary, H. Marouani, N. Issaoui and M. J. Wojcik, Impact of non-covalent interaction on FT-IR spectrum and properties of 4-methylbenzylammonium nitrate. A DFT and macular docking study, *Heliyon*, 2021, **7**, e08204.
53 M. Medimagh, N. Issaoui, S. Gatfaoui, A. S. Kazachenko, O. M. Al-Dossary, N. Kumar, H. Marouani and L. G. Bousiakoug, Investigation on the non-covalent interactions, drugs-likeness, molecular docking and chemical properties of 1,1,4,7,7-pentamethyldiethylenetriammonium trinitrate by density-functional theory, *J. King Saud Univ., Sci.*, 2023, **35**, 102645.